On Base Station Coordination in Cache- and Energy Harvesting-Enabled HetNets: A Stochastic Geometry Study

Huici Wu, *Student Member, IEEE*, Xiaofeng Tao, *Senior Member, IEEE*, Ning Zhang, *Member, IEEE*, Danyang Wang, Shan Zhang, *Member, IEEE*, and Xuemin Shen, *Fellow, IEEE*

***Abstract*— In this paper, we study the performance of base station (BS) coordination in heterogeneous networks (HetNets) with cache-enabled and renewable energy-powered small cell BSs (SBSs). Macrocell base stations (MBSs) provide basic coverage, while the SBSs, powered by harvested energy, conduct content-aware coordinated transmission to provide high data rate and further improve the network coverage. Specifically, a joint transmission strategy is performed based on the knowledge of the energy states and the cached contents of SBSs, along with the awareness of the availability of channel resources and the average received signal strength (RSS) of the corresponding link. Stochastic geometry is applied to characterize the statistics of the cell load at MBSs and SBSs, as well as the aggregated information and interference signal strength. Then, the average user capacity for the joint transmission is obtained. Additionally, the coverage probability is derived with gamma approximation for the aggregated information and interference signal strength. Analytical results reveal that the average user capacity and coverage probability can be maximized with optimal cache size, energy harvesting rate and cooperative RSS threshold. Finally, extensive numerical and simulation results are provided.**

***Index Terms*— Joint transmission, cache, energy harvesting, stochastic geometry, gamma approximation.**

I. Introduction

DRIVEN by mobile Internet-of-Things (IoT), social networks as well as the proliferation of smart devices and new applications, mobile data traffic has been growing explosively [1]. To support the ultra-high data volume, diverse low-power small cell base stations (SBSs), such as micro base stations (BSs), pico BSs, and femto BSs, are densely deployed in hotspots to provision high data rate, which results in the heterogeneous networks (HetNets) architecture [2].

With better coverage and higher throughput, HetNets are expected to be the dominant network architecture in the coming 5G era. However, the HetNets introduce serious interference due to high frequency reuse among BSs across tiers. Coordinated multi-point (CoMP) transmission has been emerged as a promising technology to alleviate the cross tier interference and further harvest the benefits of HetNets [3], [4]. But the coordination among multiple diverse BSs across tiers makes backhaul a bottleneck due to the heavy overhead signaling and information exchanges among BSs [5], [6]. Recent studies have shown that the backhaul congestions can be significantly eased by caching popular contents at the network edge such as SBSs [7], [8]. Moreover, SBSs with caching can provide low-latency services for mobile users (MUs) since it does not need to fetch the requested contents from core networks if a *cache hit* happens at SBSs.

Densely deployed SBS and large CoMP clustering can cause huge energy consumption [6], which brings heavy burden to network operators and environment. Energy harvesting (EH), which can exploit green energy from ambient environment such as wind, solar and terrestrial heat, has been leveraged into wireless networks and attracted increasing attentions [9], [10]. It is of importance to study BS coordination in cache- and EH-enabled HetNets, to provide practical insights for HetNet deployment and optimization. However, there are many challenges. i) The intermittent energy arrival with EH, causing dynamic energy states at BSs, influencing the cell load distribution of BSs, and further affecting the activation of BSs. ii) The uncertainty in satisfying users' content requests with cache, which causes mismatching of content requests at MUs and content caching at BSs. And iii) the various user quality of service requirements with different kinds of BSs. These are key factors that have great influence on the determination and formulation of cooperative BS clusters in HetNets with CoMP.

In this paper, a multi-tier orthogonal frequency division multiple access (OFDMA) based HetNet is considered, where the macrocell BSs (MBSs) provide basic coverage for MUs while the SBSs are coordinated to transmit the requested

Manuscript received August 22, 2017; revised October 31, 2017; accepted December 23, 2017. Date of publication December 29, 2017; date of current version July 13, 2018. This work was supported in part by the National Natural Science Foundation for Distinguished Young Scholars of China under Grant 61325006, in part by the National Natural Science Foundation of China under Grant 61231009, in part by the 111 Project of China under the Grant B16006, and in part by the Natural Sciences and Engineering Research Council of Canada (NSERC). The associate editor coordinating the review of this paper and approving it for publication was M. Di Renzo. *(Corresponding author: Xiaofeng Tao.)*

H. Wu and X. Tao are with the National Engineering Laboratory for Mobile Network Technologies, Beijing University of Posts and Telecommunications, Beijing 100876, China (e-mail: dailywu@bupt.edu.cn; taoxf@bupt.edu.cn).

N. Zhang is with the Department of Computing Science, Texas A&M University-Corpus Christi, Corpus Christi, TX 78412 USA (e-mail: ning.zhang@tamucc.edu).

D. Wang is with the State Key Laboratory of Integrated Service Networks, School of Telecommunications Engineering, Xidian University, Xi'an 710071, China (e-mail: danyangwang@stu.xidian.edu.cn).

S. Zhang and X. Shen are with the Department of Electrical and Computer Engineering, University of Waterloo, Waterloo, ON N2L 3G1, Canada (e-mail: s372zhan@uwaterloo.ca; sshen@uwaterloo.ca).

Color versions of one or more of the figures in this paper are available online at http://ieeexplore.ieee.org.

Digital Object Identifier 10.1109/TCOMM.2017.2788012

contents with harvested energy to provide high transmission rate and further improve the network coverage. M_0 orthogonal channels are available at MBSs and partly reused and coordinated at SBSs to serve MUs. A novel BS cooperative transmission strategy is proposed among SBSs, based on the energy states and the cached contents at SBSs, as well as the availability of channel resources and the average received-signal-strength (RSS) of the corresponding link. With the proposed cooperative strategy, the cell load distributions are obtained by means of stochastic geometry. Then, the average user capacity is analytically derived based on the characterization of the aggregated information and interference signal strength by leveraging Laplace function. Moreover, the expression for coverage probability is approximately derived with Gamma approximation. Numerical and simulation results are provided to validate the theoretical analysis and analyze the impact of network parameters. The results reveal that optimal cooperative RSS thresholds exist such that the capacity and coverage performance are maximized. The impacts of cache size and energy harvesting rate on the coverage and capacity performance depend on the cooperative RSS thresholds. With high cooperative RSS threshold, the SBSs are light-loaded and the capacity and coverage firstly improve with the increase of the cache size, the maximum number of reused channels and the energy harvesting rate at SBSs, and finally level off to optimum. For the scenario with a low cooperative RSS threshold, the SBSs are heavy-loaded and the capacity and coverage performance decrease with the increase of these SBS parameters. With an appropriate RSS threshold, the SBSs are mid-loaded and optimal cache size and energy harvesting rate exist such that the average capacity and coverage probability are maximized. However, the capacity and coverage performance firstly drop and then rise with the increase of the maximum number of channels reused at SBSs.

The remainder of this paper is organized as follows. The related work is presented in Section II. Section III introduces the system model. In Section IV, the joint transmission strategy is described and the statistics of the cell load at MBSs and SBSs are characterized. Then, the coverage probability and average capacity are analyzed in Section V. Numerical and simulation results are given in Section VI. Finally, Section VII concludes this work.

II. Related Work

CoMP has been regarded as a key technique in wireless communication system to improve network throughput, cell-edge performance, and spectral efficiency, etc., by turning interfering signals into useful signals such that the inter-cell interference is mitigated [11], [12]. With CoMP, the BSs are classified into groups [13], cooperatively serving one or more MUs. Joint transmission, one of the most advanced CoMP scenario, has been widely studied and analyzed in cellular networks [14]–[20]. Reference [14] introduced and analyzed a pairwise cooperation policy for the users at the cell borders. Reference [15] proposed a user-centric BS cooperation based on the RSS threshold and analyzed the spectral efficiency in K-tier HetNets. In [16], several heterogeneous BSs with the strongest average RSS cooperatively serve a typical MU by sorting all the BSs with their average RSS. Following Nigam *et al.* [16], extended their work to the spatio-temporal cooperation, where a second transmission attempt occurs if the first transmission fails [17]. In [19], a location-aware BS cooperation was proposed in a two-tier HetNets. As a further step, [20] proposed a novel BS cooperation strategy with the consideration of both the locations of MUs and the average RSS in non-uniform HetNets.

With cache-enabled SBSs, [21] studied the outage and data rate performance in the small cell networks with stochastic geometry. Reference [22] analyzed the throughput of HetNets with cache-enabled relays and device-to-device (D2D) pairs. To improve the network performance in cache-enabled networks, [23] proposed an interference management scheme with the assistance of cache-enabled users. Reference [24] analyzed energy efficiency (EE) of cache-enabled dense networks where cooperation is performed for downlink transmissions. A random caching based cooperative transmission was studied in [25], where the successful transmission probability is analyzed and optimized. Reference [26] considered the problem of optimal cache placement with the objective of maximizing the cache hit probability. Cooperative caching is also an efficient way in increasing the probability of successful file discovery. Reference [27] categorized the MUs into different groups according to their preferences and cooperatively share their cached content among the group. Reference [28] characterized the coverage probability and area spectral efficiency of cluster-centric content placement in a cache-enabled D2D network.

With EH employed in HetNets, [29] conducted a fundamental analysis for EH-powered HetNets by means of random walk theory and stochastic geometry. The availability region where the BSs are in active states was characterized. With discrete-time Markov modeling of the energy states of an EH-BS, the network throughput and EE of HetNets were analyzed in [30]. Furthermore, [31] studied a power-availability-aware user association in the EH-enabled small cell network. Joint transmission in wireless networks with EH-powered BSs or MUs were studied in [32] and [33]. In [32], a fractional joint transmission strategy was proposed to eliminate interference. [33] investigated the green multi-cell cooperation in HetNets facilitated with hybrid energy sources. The multicell cooperation and sleeping mechanism were performed to deal with interference and save energy, respectively.

With cache and EH employed in HetNets, BS coordination can further improve the network coverage and throughout in a more efficient way. Performance analysis in cache-enabled and EH-powered HetNets with BS coordination is vitally important to provide guidance for the practical deployment. However, existing studies either focused on the analysis of BS coordination in HetNets without considering such practical communication scenarios or studied cache-enabled and EH-powered wireless networks without considering BS coordination. In this paper, we studied the BS coordination in HetNets with cache-enabled and EH-powered SBSs. A novel joint transmission strategy with the awareness of energy states and cached contents at SBSs is performed and the network

performance in terms of average user capacity and coverage probability is analyzed in a stochastic geometry framework.

III. System Model

A. Network Model

We consider a multi-tier OFDMA based HetNet, where the MBSs provide basic coverage for MUs and the cache-enabled and EH-powered SBSs are coordinated to transmit the requested contents. A $(1+K)$-tier HetNet is assumed with one tier of MBSs overlaid with K tiers of SBSs. The distribution of MBSs are modeled as homogeneous PPP $\Phi_0 \in \mathbb{R}^2$ with spatial intensity λ_0. K tiers SBSs are deployed according to independent PPP $\Phi_k \in \mathbb{R}^2$ with intensity λ_k. The MUs are also randomly distributed as an independent PPP $\Phi_u \in \mathbb{R}^2$ with intensity λ_u. Downlink joint transmission and performance analysis are performed and developed at a typical MU located at the origin based on Slivnyak¡¯s theorem [34].

M_0 orthogonal channels with sub-bandwidth W are available at MBSs, and are randomly and uniformly allocated to the associated MUs within a cell. MUs are always associated with the nearest MBS to guarantee the basic coverage and connectivity. The channel allocated to the typical MU is defined as the reference channel. SBSs randomly reuse the channels to serve MUs according to their requirements. The maximum number of channels can be reused at an SBS in the k-th tier is M_k $(\leq M_0)$. The BSs allocate an exclusive channel to each associated MU, i.e., the MUs associated with a BS use orthogonal channels to avoid intra-cell interference. Therefore, the BS capacity, i.e., the maximum number of MUs that can be simultaneously associated with a BS, is $M_k, k = 0, \ldots, K$.

The transmission power of MBSs and SBSs, denoted as $P_k^{(\mathrm{TX})}$, are uniformly allocated among the associated MUs. Signal propagation model is considered as a composite of omni-directional path loss fading $l(d) = d^{-\alpha}$ and small-scale fading, where d is the distance between transmitter and receiver and α $(\alpha > 2)$ is the path loss exponent. For the small-scale fading, we consider independent quasi-static Rayleigh fading where the fading stays the same within one data frame and varies independently over frames.

B. Energy Harvesting Model

The MBSs are powered by the power grid and thus have sufficient energy for transmission. The SBSs, equipped with energy harvesting and storage modules, can harvest energy from environments. The SBSs in different tiers have different harvesting capabilities, i.e., energy harvesting rate and energy storage capacity. For the SBSs in the k-th tier, the energy arrival process is assumed to be identically and independently distributed (*i.i.d.*) Bernoulli process with probability μ_k and the amount of energy arrived in one time slot is denoted as Δ_k. Let Σ_k denote the required number of time slots to harvest sufficient energy for transmission, then the EH-SBSs can be silence mode without transmission if the harvested energy at SBSs is less than $\Sigma_k \Delta_k$, or work mode with transmission power $P_k^{(\mathrm{TX})}$ if the harvested energy at SBSs is above $\Sigma_k \Delta_k$.

TABLE I
Key Parameters and Notations

Symbol	Description
$\Phi_0\,(\lambda_0) \in \mathbb{R}^2$	PPP model of MBSs with density λ_0
$\Phi_k\,(\lambda_k) \in \mathbb{R}^2$	PPP model of SBSs with density λ_k
$P_0^{(\mathrm{TX})}$, $P_k^{(\mathrm{TX})}$	Transmission power of BSs in the k-th tier
M_0, M_k	BS capacity of MBSs and SBSs in the k-th tier
μ_k	Energy harvesting probability of the k-th tier
γ_k	Content popularity
T, L_k	Number of contents and the cache size of SBSs in the k-th tier
$\mathcal{B}(o, r)$	Circular area centered at o and with radius r
$\mathbb{1}(*)$	An index with value 1 if the event $*$ is true, and 0 otherwise.

C. Content Caching Model

Denote T as the number of multimedia contents. All the contents, indexed as $\mathcal{T} = [1, 2, \ldots, T]$, are considered to be with the same size S in bits and are ranked according to the request frequency. The lower indexed content has the higher popularity. Denote $\{f_{k,1}, \ldots, f_{k,T}\}$ as the popularity distribution of the contents in the k-th tier. The content popularity distribution, which is also known as the content request probability, is predicted with local or global measurements. *Zipf* distribution [22], [35] is a widely applied model with the following distribution:

$$f_{k,t} = \frac{1/t^{\gamma_k}}{\sum_{i=1}^{T} 1/i^{\gamma_k}}, t \in \mathcal{T}, \tag{1}$$

where γ_k (≥ 0) reflects the popularity distribution skewness of the k-th tier. MBSs are connected to the core network via optical fiber with high capacity. SBSs are equipped with cache modules and the cache size of SBSs in the k-th tier is L_k. Most Popular Cache (MPC) scheme is applied at SBS, i.e., the SBS in the k-th tier pre-caches the most L_k popular contents and periodically updates the cached contents.[1] MUs randomly request the contents according to the popularity distribution. The key notations are summarized as in Table I.

IV. Joint Transmission Strategy and Statistics of Cell Load

In this section, a joint transmission strategy with the awareness of the energy state, the cached contents and the channel resources at SBSs, as well as the average RSS of the corresponding link is proposed. Based on the joint transmission strategy, the statistics of cell load distributions of MBSs and SBSs are then investigated.

A. Joint Transmission Strategy

As mentioned in the network model, the typical MU is connected to the nearest MBS with the reference channel to guarantee wireless connectivity. The SBSs in the k-th tier reuse the reference channel to cooperatively transmit the typical MU's requested contents. The joint transmission is performed

[1]Locally popular content caching is considered such that the SBSs in the proximity can better perform cooperation.

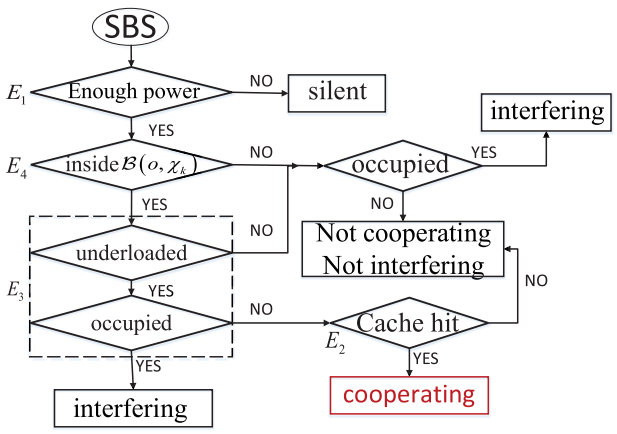

Fig. 1. Cooperative decision process of an SBS.

based on the energy states and the cached contents of SBSs, as well as the availability of channel resources and average RSS of the corresponding link. Hence, an SBS participates in the cooperation if the following four conditions are satisfied. i) *Event* E_1: the SBS has sufficient energy for transmission; ii) *Event* E_2: the requested contents of the typical MU have been cached by the SBS, i.e., cache hit happens; iii) *Event* E_3: the SBS is under-loaded and meanwhile the reference channel is not allocated to other associated MUs with the SBS; Lastly, iv) *Event* E_4: the average RSS of the corresponding link, i.e., $P_k^{(\mathrm{TX})} r^{-\alpha}$, is above the predefined cooperative RSS threshold τ_k, i.e., the SBS is located inside a circular area centered at the typical MU with radius $\chi_k = \left(\frac{P_k^{(\mathrm{TX})}}{\tau_k}\right)^{1/\alpha}$. The cooperation decision process is illustrated in Fig. 1.

From the MU's point of view, the transmission strategy performed in a user-centric manner. All the candidate SBSs (in the k-th tier) located inside $\mathcal{B}(o,\chi_k)$ (E_4) can jointly serve the typical UE if the conditions E_1, E_2 and E_3 are satisfied.

B. Statistics of Cell Load Distribution

The cell load of a BS is defined as the number of MUs that are simultaneously associated with the BS.

1) Cell Load Distribution of MBS: Define $\rho_0(m)$ as probability that m MUs are simultaneously associated with an MBS. Since MUs are associated with the nearest MBSs, the resulting network topology of the macrocell network is Poisson Voronoi (PV) tessellation. The probability density function (*pdf*) of the cell size with PV tessellation is accurately approximated by a Gamma distribution [36], [37]:

$$f(A) = \frac{(3.5\lambda_0)^{3.5}}{\Gamma(3.5)} A^{2.5} \exp(-3.5\lambda_0 A), \tag{2}$$

and probability that m_0 MUs are located in the association area of an MBS is [38], [39]:

$$\rho_0(m_0) = \frac{3.5^{3.5}\Gamma(m_0+3.5)}{m_0!\Gamma(3.5)} \frac{\left(\lambda_u/\lambda_0\right)^{m_0}}{\left(3.5+\lambda_u/\lambda_0\right)^{m_0+3.5}}, \tag{3}$$

Since the BS capacity of MBSs is M_0, the maximum cell load of an MBS is M_0. The event that an MBS is fully loaded, i.e., $m_0 = M_0$, is equivalent to the event that more than M_0 MUs are located in the association area of the MBS but only M_0 MUs are served. Thus, the cell load distribution when $m_0 < M_0$ is expressed as (3), and the probability for an MBS to be fully loaded is:

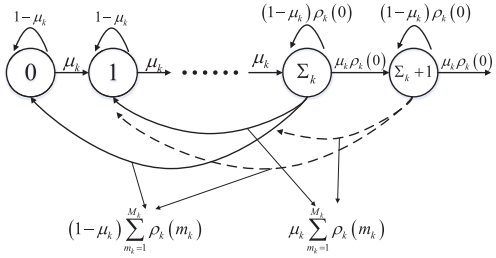

Fig. 2. Discrete-time Markov chain of the energy state at SBS.

$$\begin{aligned}\rho_0(M_0) &= \int_0^\infty \sum_{m=M_0}^{\infty} \frac{(\lambda_u A)^m e^{-\lambda_u A}}{m!} f(A)\,\mathrm{d}A \\ &\overset{(a)}{=} \int_0^\infty \frac{\gamma(M_0,\lambda_u A)}{\Gamma(M_0)} \frac{(3.5\lambda_0)^{3.5}}{\Gamma(3.5)} A^{2.5}\exp(-3.5\lambda_0 A)\,\mathrm{d}A \\ &\overset{(b)}{=} \frac{3.5^{3.5}\Gamma(M_0+3.5)}{M_0!\Gamma(3.5)} \frac{\left(\lambda_u/\lambda_0\right)^{M_0}}{\left(3.5+\lambda_u/\lambda_0\right)^{M_0+3.5}} \\ &\quad \times {}_2F_1\left(1, M_0+3.5; M_0+1; \frac{\lambda_u/\lambda_0}{3.5+\lambda_u/\lambda_0}\right), \end{aligned} \tag{4}$$

where (a) follows the Erlang distribution and (b) follows from expression [41, eq. 6.455-2]. ${}_2F_1(a,b;c;z)$ is the hypergeometric function. Note that if the BS capacity of MBSs is large enough to provide the basic connectivity for MUs, i.e., $M_0\lambda_0 \gg \lambda_u$, then $\sum_{m_0=0}^{M_0-1} \rho_0(m_0) \approx 1$ and $\rho_0(M_0) \approx 0$.

2) Cell Load Distribution of SBSs: According to the joint transmission strategy, the serving area of a random SBS x_k^i in the k-th tier is a circular area with radius χ_k, i.e., $\mathcal{B}(x_k^i, \chi_k)$. Denote $\rho_k(m_k)$ as the probability that m_k MUs are simultaneously associated with an SBS in the k-th tier. With event E_1, the SBSs without sufficient energy is zero-loaded. By modeling the energy state at SBS as Markov chain in Fig. 2, the Markov chain is stationary with $\mu_k < \Sigma_k \sum_{m_k=1}^{M_k} \rho_k(m_k)$ and the probability that an SBS has sufficient energy for transmission is $\omega_k = \frac{\mu_k}{\Sigma_k \sum_{m_k=1}^{M_k} \rho_k(m_k)}$ [30]. With E_2 and (1), the cache hit probability of the k-th tier is $\eta_k = \sum_{t=1}^{L_k} f_{k,t}$. E_3 poses a BS capacity constraint on the cell load distribution at SBSs since the maximum number of MUs the SBS x_k^i can simultaneously served is M_k. With E_4, only those MUs located in the circular serving area centered at an SBS have the opportunity to be served by the SBS. When there are n candidate MUs located inside the serving area of x_k^i, the probability of m_k cache hits happening is a binomial distribution with parameters

n and η_k, i.e.,

$$\Pr\left(m_k \text{ cache hits}\right) = \frac{n!}{m_k!\left(n-m_k\right)!}\left(\eta_k\right)^{m_k}\left(1-\eta_k\right)^{n-m_k}. \quad (5)$$

As a result, the probability that $m_k\ (< M_k)$ MUs are simultaneously served by the SBS x_k^i is:

$$\begin{aligned}
&\rho_k\left(m_k\right)\\
&= \Pr\left\{m_k \text{ MUs associated with } x_k^i\right\}\\
&= \Pr\left\{\geq m_k \text{ MUs inside } \mathcal{B}\left(x_k^i, \chi_k\right) \ \&\ m_k \text{ cache hits}\right\}\\
&\overset{(c)}{=} \sum_{n=m_k}^{\infty}\left[\begin{array}{c}\frac{\left(\pi\chi_k^2\lambda_u\right)^n\exp\left(-\pi\chi_k^2\lambda_u\right)}{n!}\\ \times\frac{n!}{m_k!\left(n-m_k\right)!}\left(\eta_k\right)^{m_k}\left(1-\eta_k\right)^{n-m_k}\end{array}\right]\\
&\overset{(d)}{=} \left(\pi\chi_k^2\eta_k\lambda_u\right)^{m_k}\frac{\exp\left(-\pi\chi_k^2\eta_k\lambda_u\right)}{m_k!}, \qquad (6)
\end{aligned}$$

where (c) holds due to the PPP distribution of MUs and the binomial distribution of caching and (d) follows the Taylor expansion of exponential distribution. The probability for an SBS to be fully loaded, i.e., $m_k = M_k$, is

$$\begin{aligned}
\rho_k\left(M_k\right) &= \Pr\left\{M_k \text{ MUs associated with } x_k^i\right\}\\
&= \sum_{m=M_k}^{\infty}\frac{\left(\pi\chi_k^2\eta_k\lambda_u\right)^m\exp\left(-\pi\chi_k^2\eta_k\lambda_u\right)}{m!} \qquad (7)
\end{aligned}$$

Combining with the cell load distribution, the probability for an SBS in the k-th tier to have sufficient energy can be expressed as:

$$\omega_k = \frac{\mu_k}{\left[1-\exp\left(-\pi\chi_k^2\eta_k\lambda_u\right)\right]\Sigma_k}. \qquad (8)$$

Note that with the Markov modeling of energy state of SBSs, the Markov chain will not be stationary and the SBS will always have enough energy for transmission if the energy arrival rate exceeds the energy consumption rate, i.e., $\mu_k \geq \left[1-\exp\left(-\pi\chi_k^2\eta_k\lambda_u\right)\right]\Sigma_k$. Therefore, when the SBSs are non zero-loaded with very high probability, the harvested energy will be consumed quickly and the probability ω_k decreases. By setting a higher cooperative RSS threshold or a lower cache size at SBS, the probability that an SBS is zero-loaded increases and thus the stored energy at SBSs as well as the probability that the SBSs have sufficient energy for transmission increases. Overall, we can see from (6)-(8) that the cooperative RSS thresholds τ_k, the cache size L and the maximum number of channels M_k jointly influence the cell load distribution of SBSs, which further affects the energy states at SBSs.

V. Analysis of Average User Capacity and Coverage Probability

In this section, the statistics of the aggregated information and interference signal strength with the proposed joint transmission scheme are studied by means of Laplace function. Then, the average capacity achievable at the typical MU is obtained. Based on the statistics, the coverage probability is approximately derived by leveraging Gamma approximation for the distributions of the aggregated information and interference signal strength.

A. Statistics of the Signal and Interference Strength

Denote x_0 as the nearest MBS to the typical MU with distance $r_0 = \|x_0\|$, then the *pdf* of r_0 is $f_{r_0}(r) = 2\pi\lambda_0 r e^{-\pi\lambda_0 r^2}$. Denote S_k and I_k as the aggregated information and interference signal strength received from the SBSs in the k-th tier. With non-coherent transmission at the cooperative BSs, the received signal-to-interference-plus-noise ratio (SINR) at the typical MU is

$$\text{SINR} = \frac{S_0 + \sum_{k=1}^{K} S_k}{\sum_{k=0}^{K_1+K_2} I_k + \sigma^2}, \qquad (9)$$

where

$$S_0 = \frac{P_0^{(\text{TX})}}{m_0+1}\|x_0\|^{-\alpha}h_{x_0}, m_0 \leq M_0 - 1, \qquad (10)$$

and

$$I_0 = \sum_{x\in\Phi_0\setminus\mathcal{B}(o,r_0)}\mathbb{1}\left(\text{occupied}\right)\frac{P_0^{(\text{TX})}}{m_x}\|x\|^{-\alpha}h_x, \qquad (11)$$

are the received information signal strength and aggregated interference strength from MBSs. m_0 and m_x are the number of *other* MUs associated with the nearest MBS x_0 and the interfering MBS x, respectively. h_{x_0} and h_x are the channel fading, which are exponentially distributed with unit mean. $\mathbb{1}\left(\text{occupied}\right)$ is the indicator function, where $\mathbb{1}\left(\text{occupied}\right) = 1$, if the MBS x have reused the reference channel to serve an MU, and $\mathbb{1}\left(\text{occupied}\right) = 0$, otherwise. For an SBS located at $x_k \in \Phi_k \cap \mathcal{B}(o, \chi_k)$ and with m_{x_k} *other* associated MUs, it can join to transmit the typical MU's data if it satisfies the cooperation conditions E_1, E_2 and E_3. Therefore, the aggregated information signal strength received from the SBSs in the k-th tier is expressed as:

$$S_k = \sum_{x_k\in\Phi_k\cap\mathcal{B}(o,\chi_k)}\mathbb{1}\left(E_1 \& E_2 \ \&\ E_3\right)\frac{P_k^{(\text{TX})}}{m_{x_k}+1}\|x_k\|^{-\alpha}h_{x_k}. \qquad (12)$$

The SBSs in the k-th tier interfere with the typical MU if the reference channel is reused to serve other MUs. Thus, the aggregated interference strength from the k-th tier is

$$I_k = \sum_{x_k\in\Phi_k}\mathbb{1}\left(E_1 \ \&\ \text{occupied}\right)\frac{P_k^{(\text{TX})}}{m_{x_k}}\|x_k\|^{-\alpha}h_{x_k} \qquad (13)$$

In the following, we provide the Laplace function of S_k and I_k to characterize the statistics of received information and interference signal strength.

Lemma 1: The Laplace function of S_0 conditioned on r_0 is

$$\mathcal{L}_{S_0}\left(t|r_0\right) = \rho_0\left(M_0\right) + \sum_{m_0=0}^{M_0-2}\rho_0\left(m_0+1\right)\frac{\frac{m_0+1}{P_0^{(TX)}}r_0^{\alpha}}{t+\frac{m_0+1}{P_0^{(TX)}}r_0^{\alpha}}. \qquad (14)$$

Proof: Please refer to Appendix A-A. ∎

For an SBS in the k-th tier with m_k ($< M_k$) *other* associated MUs, the reference channel is available to the typical MU if none of the m_k MUs is served with the reference channel. Thus, the probability that the reference channel is available to the typical MU is

$$\frac{(M_0-1)\ldots(M_0-m_k)}{M_0\,(M_0-1)\ldots(M_0-m_k+1)}=\frac{M_0-m_k}{M_0}. \quad (15)$$

When the reference channel is not available at the SBS or the requested contents is not cached, the SBS will not participate in cooperation. Thus, the probability that an SBS, with sufficient energy, located inside $\mathcal{B}(o,\chi_k)$ in the k-th tier can participate in transmitting the typical MU's data is $\nu_k = \eta_k \sum_{m_k=0}^{M_k-1} \rho_k(m_k+1)\frac{M_0-m_k}{M_0}$.

Lemma 2: The Laplace function of the aggregated information signal strength S_k is

$$\mathcal{L}_{S_k}(t)=\exp\left\{\begin{array}{l}-\pi\lambda_k\omega_k\chi_k^2\eta_k\sum\limits_{m_k=0}^{M_k-1}\rho_k(m_k+1)\\ \times\frac{M_0-m_k}{M_0}\left(1-\mathcal{Z}_1\left(\frac{m_k+1}{t\tau_k}\right)\right)\end{array}\right\}, \quad (16)$$

where

$$\mathcal{Z}_1(x)=\frac{2x}{\alpha+2}\times{}_2F_1\left(1,1+\frac{2}{\alpha};2+\frac{2}{\alpha};-x\right), \quad (17)$$

Proof: Please refer to Appendix A-B. ∎

The MBSs randomly and uniformly distribute the channels to the associated MUs. Thus, the probability that an MBS with m_0 other associated MUs reuses the reference channel and interferes with the typical MU is $\frac{m_0}{M_0}$.

Lemma 3: The Laplace function of the aggregated interference strength from MBSs is

$$\mathcal{L}_{I_0}(t|r_0)=\exp\left\{-\pi\lambda_0 r_0^2\sum_{m_0=1}^{M_0}\rho_0(m_0)\frac{m_0}{M_0}\mathcal{Z}_2\left(\frac{m_0 r_0^{\alpha}}{tP_0^{(TX)}}\right)\right\}, \quad (18)$$

where

$$\mathcal{Z}_2(x)=\frac{2x^{-1}}{\alpha-2}\times{}_2F_1\left(1,1-\frac{2}{\alpha};2-\frac{2}{\alpha};-x^{-1}\right). \quad (19)$$

Proof: Please refer to Appendix A-C. ∎

For the interfering SBSs in the k-th tier with enough energy, they interfere with the typical MU if they have served other MUs with the reference channel. The probability that the reference channel is reused at an SBS with m_k associated MU is

$$\frac{m_k\,(M_0-1)\ldots(M_0-m_k+1)}{M_0\,(M_0-1)\ldots(M_0-m_k+1)}=\frac{m_k}{M_0}. \quad (20)$$

Lemma 4: The Laplace function of the aggregated interference strength from the SBSs in the k-th tier is

$$\mathcal{L}_{I_k}(t)=\exp\left\{\begin{array}{l}-\frac{2\pi\omega_k\lambda_k}{\alpha M_0}\left(tP_k^{(TX)}\right)^{2/\alpha}\times\\ B\left(\frac{2}{\alpha},1-\frac{2}{\alpha}\right)\sum\limits_{m_k=1}^{M_k}\rho_k(m_k)\,m_k^{1-2/\alpha}\end{array}\right\} \quad (21)$$

where $B\left(\frac{2}{\alpha},1-\frac{2}{\alpha}\right)$ is the Beta function.

Proof: Please refer to Appendix A-D. ∎

From the cell load distribution (6) and the Laplace function (16), we can see that with the decrease of the cooperative RSS threshold (i.e., with the expansion of the cooperative area), the number of candidate cooperative SBSs as well as the probability of heavy-loaded SBSs increase, while the probabilities ν_k and ω_k decrease, which results in a tradeoff between the number of candidate SBSs and the cooperation probability of a candidate SBS. Similarly, with the increasing of the cache size at SBSs, there is a tradeoff between the cache hit probability η_k and the joint probability $\omega_k\sum_{m_k=0}^{M_k-1}\rho_k(m_k+1)$. For the aggregated interference strength I_k, a tradeoff between the probability for having sufficient energy ω_k and the interfering probability $\sum_{m_k=1}^{M_k}\rho_k(m_k)$ exists with the varying of the cooperative RSS threshold and the cache size. To investigate the influence of network parameters, we then theoretically analyze the average user capacity and coverage probability to study the capacity and coverage performance of the HetNets.

B. Average Capacity Analysis

When the cooperative BSs adopts appropriate adaptive modulation and coding, the average Shannon capacity of the multiple-input single-output channel between the cooperative BSs and the typical MU is

$$\mathcal{R}_c=W\mathbb{E}\left[\ln(1+\mathrm{SINR})\right], \quad (22)$$

in nats/s.

Theorem 1: In the cache-enabled EH-powered HetNets with the performed BS cooperation strategy, the average user capacity is

$$\mathcal{R}_c=W\int_0^{\infty}\left(\frac{e^{-\sigma^2 t}}{t}\prod_{k=1}^{K}\mathcal{L}_{I_k}(t)\int_0^{\infty}\left(\mathcal{L}_{I_0}(t|r)\times\left(1-\mathcal{L}_{S_0}(t|r)\prod_{k=1}^{K}\mathcal{L}_{S_k}(t)\right)\right)f_{r_0}(r)\,\mathrm{d}r\right)\mathrm{d}t \quad (23)$$

Proof: Applying the result as in [41], the average capacity per frequency band (also known as spectral efficiency) at the typical MU is expressed as:

$$\begin{aligned}&\mathbb{E}\left[\ln(1+\mathrm{SINR})\right]\\ &=\mathbb{E}_r\left[\int_0^{\infty}\frac{\prod_{k=0}^{K}\mathcal{L}_{I_k}(t)\left(1-\prod_{k=0}^{K}\mathcal{L}_{S_k}(t)\right)}{t}e^{-\sigma^2 t}\mathrm{d}t\right]\\ &\overset{(e)}{=}\int_0^{\infty}\int_0^{\infty}\left(\begin{array}{c}\mathcal{L}_{I_0}(t|r)\prod_{k=1}^{K}\mathcal{L}_{I_k}(t)-\mathcal{L}_{I_0}(t|r)\\ \times\mathcal{L}_{S_0}(t|r)\prod_{k=1}^{K}\mathcal{L}_{I_k}(t)\,\mathcal{L}_{S_k}(t)\end{array}\right)\frac{e^{-\sigma^2 t}}{t}\mathrm{d}t\,f_{r_0}(r)\,\mathrm{d}r\end{aligned} \quad (24)$$

where (e) holds due to the independence of the variables. Substituting (24) into (22), the average capacity (23) is obtained. ∎

$$\mathbb{E}[S_k] = \frac{2\pi\lambda_k\omega_k\eta_k P_k^{(\mathrm{TX})}}{M_0(\alpha-2)}\left(1-\chi_k^{2-\alpha}\right)\sum_{m_k=0}^{M_k-1}\rho_k(m_k+1)\frac{M_0-m_k}{m_k+1},$$

$$\mathbb{V}[S_k] = \frac{\pi\lambda_k\omega_k\eta_k\left(P_k^{(\mathrm{TX})}\right)^2}{2M_0(\alpha-1)}\left(1-\chi_k^{2-2\alpha}\right)\sum_{m_k=0}^{M_k-1}\rho_k(m_k+1)\frac{M_0-m_k}{(m_k+1)^2}. \tag{25}$$

$$\mathbb{E}[I_0|r_0] = r_0^{2-\alpha}\frac{2\pi\lambda_0 P_0^{(\mathrm{TX})}}{M_0(\alpha-2)}(1-\rho_0(0)),\ \mathbb{V}[I_0|r_0] = r_0^{2-2\alpha}\frac{\pi\lambda_0\left(P_0^{(\mathrm{TX})}\right)^2}{2(\alpha-1)M_0}\sum_{m=1}^{M_0}\frac{\rho_0(m)}{m}. \tag{26}$$

$$\mathbb{E}[I_k] = \frac{2\pi\lambda_k\omega_k P_k^{(\mathrm{TX})}}{M_0(\alpha-2)}(1-\rho_k(0)),\ \mathbb{V}[I_k] = \frac{\pi\lambda_k\omega_k\left(P_k^{(\mathrm{TX})}\right)^2}{2(\alpha-1)M_0}\sum_{m_k=1}^{M_k}\frac{\rho_k(m_k)}{m_k}. \tag{27}$$

C. Coverage Probability Analysis

When the cooperative BSs serve the typical MU at a fixed rate, outage can occur and the typical MU cannot reliably decode the signals if the received SINR at the typical MU is below the predefined threshold. Thus, we define the coverage probability, also known as successful transmission probability, to measure the coverage performance of the HetNets. Mathematically, the coverage probability is the complementary cumulative distribution function (CCDF) of the received SINR, i.e.,

$$\mathcal{P}_{\mathrm{cov}}(\beta) = \Pr[\mathrm{SINR}\geq\beta], \tag{28}$$

where β is the predefined coverage threshold.

Theorem 2: In the cache-enabled and EH-powered HetNets with the performed BS cooperation, the coverage probability of a typical MU is approximately expressed as:

$$\begin{aligned}\mathcal{P}_{\mathrm{cov}}(\beta) \approx{}& \sum_{m_0=0}^{M_0-2}\rho_0(m_0+1)\int_0^\infty \exp\left\{-r^2\sum_{k=0}^{K}\lambda_k u_k\right\} f_{r_0}(r)\,\mathrm{d}r \\ &+ \sum_{m_0=0}^{M_0-2}\rho_0(m_0+1)\int_0^\infty \frac{\Gamma(\kappa_S+\kappa_Z)\varphi^{\kappa_S}}{\Gamma(\kappa_S)\Gamma(\kappa_Z)} \\ &\times\left[\frac{1}{\kappa_Z}\left(\mathcal{Z}_3(1)-\mathcal{Z}_3\left(1+\frac{\beta\theta_Z(m_0+1)}{P_0^{(TX)}r^{-\alpha}}\right)\right)\right. \\ &\left.+\frac{1}{\kappa_S}\left(\mathcal{Z}_4(\varphi)-\mathcal{Z}_4\left(\varphi+\frac{\beta\theta_Z(m_0+1)}{P_0^{(TX)}r^{-\alpha}}\right)\right)\right] f_{r_0}(r)\,\mathrm{d}r,\end{aligned} \tag{29}$$

where u_0 and u_k are expressed as:

$$\begin{aligned}u_0 &= \pi\sum_{m_0=1}^{M_0}\frac{m_0}{M_0}\rho_0(m_0)\mathcal{Z}_2\left(\frac{m_0}{\beta(m_0+1)}\right), \\ u_k &= \frac{2\pi\omega_k\beta^{2/\alpha}(m_0+1)^{2/\alpha}}{\alpha M_0}\left(\frac{P_k^{(TX)}}{P_0^{(TX)}}\right)^{2/\alpha} \\ &\quad\times B\left(\frac{2}{\alpha},1-\frac{2}{\alpha}\right)\sum_{m_k=1}^{M_k}\rho_k(m_k)m_k^{1-2/\alpha},\end{aligned} \tag{30}$$

respectively. φ is defined as $\varphi=\frac{\beta\theta_Z}{\theta_S}$. κ_S, θ_S and κ_Z, θ_Z are expressed as (43) and (46) in Appendix B with the mean and variance of S_k and I_k shown as (25)-(27) at the top of the page. $\mathcal{Z}_3(x)$ and $\mathcal{Z}_4(x)$ are respectively expressed as:

$$\mathcal{Z}_3(x) = \frac{{}_2F_1\left(1,\kappa_S+\kappa_Z;\kappa_Z+1;\frac{x}{(x+\varphi)}\right)}{(x+\varphi)^{\kappa_S+\kappa_Z}}, \tag{31}$$

and

$$\mathcal{Z}_4(x) = \frac{{}_2F_1\left(1,\kappa_S+\kappa_Z;\kappa_S+1;\frac{x-\frac{\beta\theta_Z(m_0+1)}{P_0^{(TX)}r_0^{-\alpha}}}{1+x}\right)}{(1+x)^{(\kappa_S+\kappa_Z)}}. \tag{32}$$

Proof: Please refer to Appendix B. ∎

Although (23) and (29) are not in closed-form, the Laplace functions can be easily calculated by MatLab, and therefore the coverage probability and average user capacity can be numerically evaluated. Moreover, from the above analysis, we can see that for a dominant cooperating or interfering SBS (i.e., the SBSs located inside $\mathcal{B}(o,\chi_k)$.) with uniform power allocation, the average cooperating transmission power is

$$\omega_k\eta_k\frac{P_k^{(\mathrm{TX})}}{M_0}\sum_{m=0}^{M_k-1}\rho_k(m+1)\frac{M_0-m}{m+1}, \tag{33}$$

and the average interfering transmission power is

$$\omega_k\frac{P_k^{(\mathrm{TX})}}{M_0}\sum_{m=1}^{M_k}\rho_k(m). \tag{34}$$

Thus, there exists a tradeoff between the average cooperating transmission power and the average interfering transmission power at the dominant SBSs. The cooperative RSS thresholds, the cache size at SBSs, and the energy harvesting capability are key parameters that influence the average cooperating and interfering transmission power.

VI. Numerical Results

In this section, we provide numerical and simulation results to evaluate the average user capacity and coverage probability in a two-tier HetNet, where the MBSs are overlaid by one tier of cache-enabled and EH-powered SBSs. Simulation results

TABLE II
SIMULATION PARAMETERS

Parameter	Value
λ_0, λ_1 and λ_u	$\frac{1}{\pi 500^2}$, $\frac{10}{\pi 500^2}$, $\frac{20}{\pi 500^2}$
M_0, M_1	50, 10
$P_0^{(\mathrm{TX})}$, $P_1^{(\mathrm{TX})}$	37dBm, 30dBm
T, L_1 γ_1	200, 10, 0.8
μ_1 Δ_1, Σ_1	0.5, 1, 5
α	4
W	10MHz
σ^2 (10MHz)	-104dBm

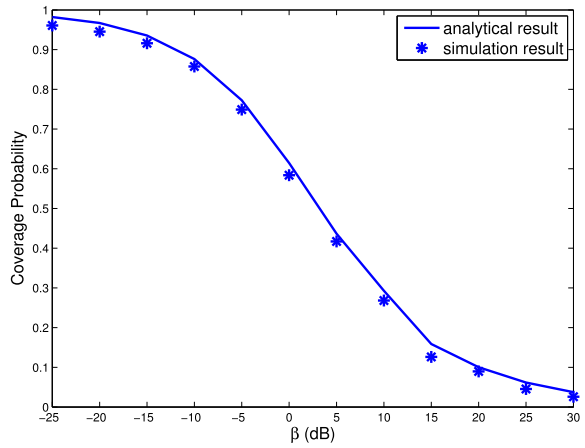

Fig. 3. Coverage probability with respect to the coverage threshold β, when $\tau_1 = -60$dBm.

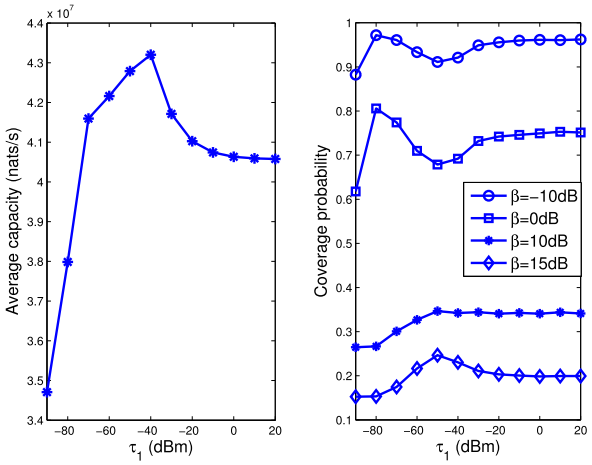

Fig. 4. Average capacity and coverage probability with respect to τ_1.

are obtained with Monte Carlo methods in a circular area with radius 5km. The detailed simulation parameters are given as in Table II unless otherwise specified.

Firstly, the simulation and numerical results are compared in Fig. 3. The gap between the analytical and the simulation result is due to the Gamma approximation for the distributions of aggregated information and interference signal strength.

A. The Impact of Cooperative RSS Threshold

Fig. 4 shows the impact of the cooperative RSS thresholds (τ_1). It can be seen that when τ_1 approximately equals to or less than -90 dBm, the SBSs are full-loaded with probability 1 and almost zero-loaded when τ_1 approaches to or above 0 dBm. Moreover, optimal cooperative RSS threshold exists such that the average user capacity and coverage probability are maximized. This is due to the tradeoff between the cooperative probability of an SBS and the number of candidate SBSs, as discussed in Sec. V-A. With low τ_1, the area for candidate SBSs is large and the load at SBSs with sufficient energy is heavy, which results in a low probability of sufficient energy at SBSs. As a result, very few SBSs can participate in the cooperation while the SBSs with sufficient energy generate interference with almost probability 1, which causes low data rate and coverage probability. As τ_1 increases, although the area for the candidate cooperative SBSs shrinks and the number of the candidate SBSs decreases, the probability that an SBS is cooperative and the probability of sufficient energy increases. Hence, the aggregated information signal strength firstly increases and then decreases with the increase of τ_1. Similarly, the interfering probability of an SBS reduces sharply with the increase of τ_1 and thus the average aggregated interference strength drops rapidly. As a result, the average SINR received at the typical MU firstly rises and then drops and there is an optimal τ_1 maximizing the average capacity.

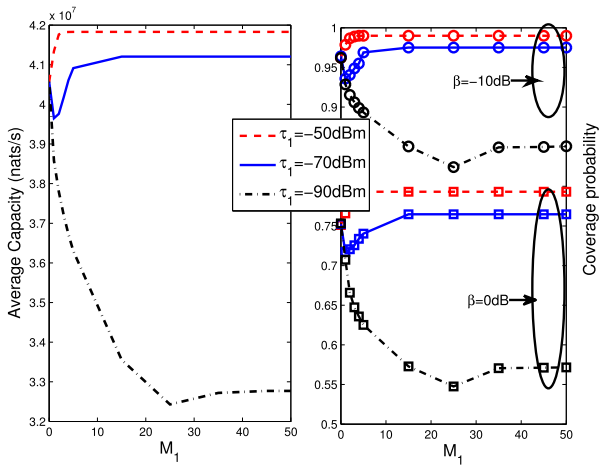

Fig. 5. Average capacity and coverage probability with respect to M_1.

Combining with Eqs. (25)-(27), we can see that the variance of SINR changes with the increase of τ_1. When τ_1 is large enough, the SBSs neither join cooperation nor interfere with the typical MU and the resulting SINR is almost SINR $= \frac{S_0}{I_0+\sigma^2}$ with very high probability. In such cases, the variance of SINR is quite small. Increasing τ_1, the average cell load at the SBSs varies from M_1 to 0 and the number of cooperative SBSs firstly increases and then decreases, leading to the variance of SINR an peak function with respect to τ_1. Combining with the result for the average SINR, the coverage probability $\mathcal{P}_{\mathrm{cov}}(\beta) = \Pr\{\mathrm{SINR} > \beta\}$ will have a minimum value if the coverage threshold is small, as show in Fig. 4.

B. The Impact of Channel Reuse

To investigate the influence of the channel reuse among tiers, Fig. 5 shows the average capacity and coverage probability with respect to the maximum number of channels reused at SBS, i.e., M_1. With fixed cooperative RSS threshold and cache

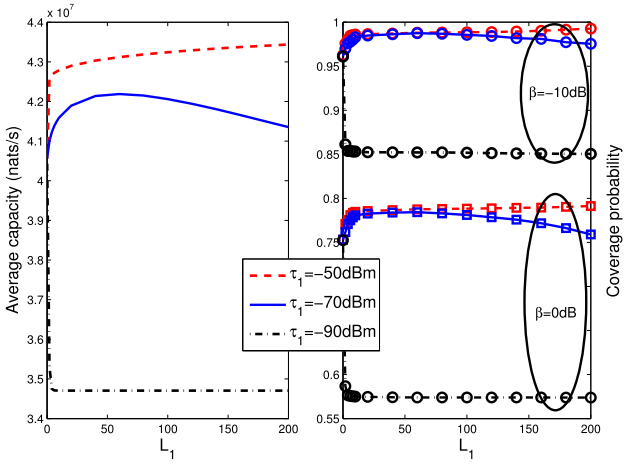

Fig. 6. Average capacity and coverage probability with respect to L_1.

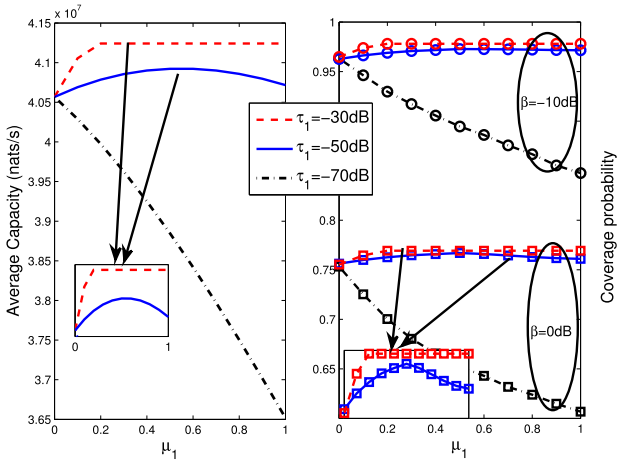

Fig. 7. Average capacity and coverage probability with respect to μ.

size at SBSs, the probability of zero-loading at SBSs as well as the probability for having sufficient energy at SBSs is determined. If the average cooperating transmission power (33) is above the interfering transmission power (34) at a dominant SBS, the network performance will be improved. As shown in Fig. 5, with a low threshold τ_1, e.g., $\tau_1 = -70$ dBm, the zero-load probability is very small (e.g., $\rho_1(0) = 0.057$) if more than one channel is reused at the SBS. In this case, the aggregated interference strength (I_1) dominates the aggregated information signal strength (S_1) when M_1 increases from 0 to 1, and the performance decreases. However, S_1 increases with M_1 while I_1 almost keeps unchanged, and the performance improves. With an appropriate cooperative RSS threshold, e.g., $\tau_1 = -50$ dBm, the zero-load probability is $\rho_1(0) = 0.75$. In this case, the signal strength S_1 always dominates the interference strength I_1 and the average capacity as well as the coverage performance improves with M_1.

C. The Impact of Cache Size

Fig. 6 shows the impact of the cache size of SBSs. It can be seen that an optimal cache size maximizing the average user capacity and coverage probability exists with appropriate cooperative RSS threshold. When τ_1 is too small, e.g., $\tau_1 = -90$ dBm, the SBSs will be full-loaded if cache hit happens and (34) > (33) $+\delta$[2] always establishes. As a result, I_1 always dominates S_1 and the network performance decreases. When $\tau_1 = -70$ dBm, the SBSs are mid-loaded. (34) < (33) $+\delta$ holds when the cache size L_1 is below certain value and (34) > (33) $+\delta$ holds when L_1 is above the value, which results in the optimal cache size at SBSs. When the cooperative RSS threshold is $\tau_1 = -50$ dBm or more high, the SBSs are light-load and (34) < (33) $+\delta$ always follows. In this case, the network performance improves with L_1 and finally levels off.

D. The Impact of Energy Harvesting

Fig. 7 shows the impact of the energy harvesting rate μ. It can be seen that the network performance decreases when $\tau_1 = -70$ dBm and levels off to maximum when $\tau_1 = -30$ dBm. Moreover, there exists an optimal energy harvesting rate when $\tau_1 = -50$ dBm. As we can see from (8) that with fixed τ_1 and L_1, the probability for having sufficient energy at an SBS is determined by μ. With heavy-loaded SBSs (e.g., $\tau_1 = -70$ dBm), the SBSs can hardly join cooperation while they introduce severe interference with more energy harvested. With mid-loaded SBSs (e.g., $\tau_1 = -50$ dBm), the capacity and coverage firstly increases because the increased information signal strength dominates the interference strength. However, due to the limited number of cooperative SBSs, the performance finally decreases due to the increasing of interference strength. With light-loaded SBSs (e.g., $\tau_1 = -30$ dBm), the network performance improves due to the limited number of interfering SBSs and levels off because the cooperative SBSs tend to have sufficient energy with probability 1, even increasing the energy harvesting rate.

VII. Conclusion

In this paper, we have proposed a joint transmission strategy for the cache-enabled and renewable energy-powered HetNets, to provide high transmission data rate and further improve the network coverage performance. Furthermore, we have theoretically analyzed the coverage probability and average capacity with stochastic geometry approach and Gamma approximation. Numerical results have been provided to validate the theoretical analysis and revealed that there exists an optimal cooperative RSS threshold for maximizing the coverage and capacity performance. Moreover, with an appropriate cooperative RSS threshold around the optimal cooperative RSS threshold, the SBSs are mid-loaded. In such a scenario, i) the optimal cache size and energy harvesting rate exist in maximizing the average capacity and coverage probability, and ii) the average capacity and coverage probability firstly decrease and then increase with the increase of the maximum number of channels available at SBSs, and finally level off to optimum performance. These results provide insights for the deployment and operation of cache-enabled and energy harvesting-powered SBSs in HetNets. The proposed BS coordination strategy can be widely applied in practice, especially for the

[2] δ is a compensation for the interfering SBSs except the dominant interfering SBSs.

energy-constraint and backhaul-limited networks, to enhance the coverage and service quality for MUs, in a cost-effective way. For the future work, we will consider more realistic channel models [42] and investigate the optimal cooperative RSS threshold and cache size at SBSs, to further enhance the user experience and improve the coverage performance.

APPENDIX A
PROOF OF LEMMAS

A. Proof of Lemma 1

The distribution of S_0 conditioned on r_0 and m_0 is

$$f_{S_0}(s|r_0,m_0)=\frac{m_0+1}{P_0^{(\mathrm{TX})}}r_0^{\alpha}f_h\left(\frac{m_0+1}{P_0^{(\mathrm{TX})}}r_0^{\alpha}s\right).$$

Then, the Laplace function of S_0 conditioned on r_0 is obtained by applying the Laplace transform, i.e.,

$$\begin{aligned}&\mathcal{L}_{S_0}(t|r_0)\\&=\mathbb{E}_{S_0}\left(e^{-tS_0}\right)\\&\overset{(f)}{=}\rho_0(M_0)+\int_0^{\infty}e^{-st}\sum_{m_0=0}^{M_0-2}\rho_0(m_0+1)\frac{m_0+1}{P_0^{(\mathrm{TX})}}r_0^{\alpha}e^{-\frac{m_0+1}{P_0^{(\mathrm{TX})}}r_0^{\alpha}s}\mathrm{d}s\\&=\rho_0(M_0)+\sum_{m_0=0}^{M_0-2}\rho_0(m_0+1)\frac{\frac{m_0+1}{P_0^{(\mathrm{TX})}}r_0^{\alpha}}{t+\frac{m_0+1}{P_0^{(\mathrm{TX})}}r_0^{\alpha}}\end{aligned}\tag{35}$$

where (f) is the result of the fact that $S_0=0$ when the nearest MBS is full-loaded and will not serve the typical MU.

B. Proof of Lemma 2

With the definition of Laplace transform, the Laplace function of S_k is

$$\begin{aligned}&\mathcal{L}_{S_k}(t)\\&=\mathbb{E}_{S_k}\left[e^{-tS_k}\right]\\&\overset{(g)}{=}\exp\left\{-2\pi\lambda_k\omega_k\int_0^{\chi_k}\left(1-\mathbb{E}_h\left[e^{-\mathbb{1}(E_2\&E_3)t\frac{P_k^{(\mathrm{TX})}}{m_k+1}r^{-\alpha}h}\right]\right)r\mathrm{d}r\right\}\\&\overset{(h)}{=}\exp\left\{-2\pi\lambda_k\omega_k\int_0^{\chi_k}\left(\nu_k-\eta_k\sum_{m_k=0}^{M_k-1}\frac{M_0-m_k}{M_0}\right.\right.\\&\qquad\left.\left.\frac{\rho_k(m_k+1)}{1+t\frac{P_k^{(\mathrm{TX})}}{m_k+1}r^{-\alpha}}\right)r\mathrm{d}r\right\}\\&=\exp\left\{\begin{array}{l}-\pi\lambda_k\chi_k^2\eta_k\omega_k\sum_{m_k=0}^{M_k-1}\rho_k(m_k+1)\frac{M_0-m_k}{M_0}\times\\\left(1-\frac{2}{\alpha+2}\frac{m_k+1}{t\tau_k}\times\right.\\\left.{}_2F_1\left(1,1+\frac{2}{\alpha};2+\frac{2}{\alpha};-\frac{m_k+1}{t\tau_k}\right)\right)\end{array}\right\}\end{aligned}\tag{36}$$

where (g) follows the probability generation function of PPP [34] and (h) holds because the SBS participates in cooperation with probability ν_k and $h\sim\exp\{1\}$. Thus,

$$\mathbb{E}_h\left[e^{-t\frac{P_k^{(\mathrm{TX})}}{m_k+1}r^{-\alpha}h}\right]=\frac{1}{1+t\frac{P_k^{tx}}{m_k+1}r^{-\alpha}}.$$

C. Proof of Lemma 2

The interfering macro BSs are located outside $\mathcal{B}(o,r_0)$.

$$\begin{aligned}&\mathcal{L}_{I_0}(t|r_0)\\&=\mathbb{E}_{I_0}\left[e^{-t\sum\limits_{x\in\Phi_0\setminus\mathcal{B}(o,r_0)}\mathbb{1}(\text{occupied})\frac{P_0^{(\mathrm{TX})}}{m_x}\|x\|^{-\alpha}h_x}\right]\\&\overset{(i)}{=}\exp\left\{-2\pi\lambda_0\int_{r_0}^{\infty}\left(\begin{array}{c}1-\rho_0(0)-\sum_{m_0=1}^{M_0}\rho_0(m_0)\\\times\left(\frac{m_0}{M_0}\frac{1}{1+\frac{tP_0^{(\mathrm{TX})}}{m_0}r^{-\alpha}}+1-\frac{m_0}{M_0}\right)\end{array}\right)r\mathrm{d}r\right\}\\&=\exp\left\{\begin{array}{c}-\pi\lambda_0r_0^2\sum_{m_0=1}^{M_0}\rho_0(m_0)\frac{m_0}{M_0}\frac{2}{(\alpha-2)}\frac{tP_0^{(\mathrm{TX})}}{m_0r_0^{\alpha}}\\\times{}_2F_1\left(1,1-\frac{2}{\alpha};2-\frac{2}{\alpha};-\frac{tP_0^{(\mathrm{TX})}}{m_0r_0^{\alpha}}\right)\end{array}\right\}\end{aligned}\tag{37}$$

where (i) follows the fact that the MBS is zero-loaded with probability $\rho_0(0)$ and the MBS with m_0 associated MUs reuse the reference channel with probability $\frac{m_0}{M_0}$.

D. Proof of Lemma 3

For the interference caused by PG-SBS, the Laplace function of I_k is (38), as shown at the top of the next page, where (j) is the result of the following integral.

$$\begin{aligned}&2\int_0^{\infty}\left(1-\frac{1}{1+\frac{tP_k^{(\mathrm{TX})}}{m_k}r^{-\alpha}}\right)r\mathrm{d}r\\&\overset{u=\left(\frac{m_k}{tP_k^{(\mathrm{TX})}}\right)^{2/\alpha}r^2}{=}\left(\frac{tP_k^{(\mathrm{TX})}}{m_k}\right)^{2/\alpha}\int_0^{\infty}\left(1-\frac{u^{\frac{\alpha}{2}}}{1+u^{\frac{\alpha}{2}}}\right)\mathrm{d}u\\&\overset{v=u^{\frac{\alpha}{2}}}{=}\frac{2}{\alpha}\left(\frac{tP_k^{(\mathrm{TX})}}{m_k}\right)^{2/\alpha}B\left(\frac{2}{\alpha},1-\frac{2}{\alpha}\right)\end{aligned}\tag{39}$$

APPENDIX B
PROOF OF THEOREM 2

According to the definition of the coverage probability, $\mathcal{P}_{\mathrm{cov}}(\beta)$ is expressed as:

$$\mathcal{P}_{\mathrm{cov}}(\beta)=\Pr\left[S_0+\sum_{k=1}^{K}S_k\geq\beta\left(I_0+\sum_{k=1}^{K}I_k+\sigma^2\right)\right].\tag{40}$$

$$\begin{aligned}\mathcal{L}_{I_k}(t) &= \mathbb{E}\left[e^{-t\sum\limits_{x_k\in\Phi_k}\mathbb{1}(E_1\&\text{occupied})\frac{P_k^{(\mathrm{TX})}}{m_{x_k}}\|x_k\|^{-\alpha}h_{x_k}}\right]\\ &= \exp\left\{-2\pi\lambda_k\omega_k\int_0^{\infty}\left(\begin{array}{c}1-\rho_k(0)-\sum\limits_{m_k=1}^{M_k}\rho_k(m_k)\\ \times\left(\frac{m_k}{M_0}\frac{1}{1+\frac{tP_k^{(\mathrm{TX})}}{m_k}r^{-\alpha}}+1-\frac{m_k}{M_0}\right)\end{array}\right)r\mathrm{d}r\right\}\\ &\overset{(j)}{=}\exp\left\{-\frac{2\pi\lambda_k}{\alpha M_0}\left(tP_k^{(\mathrm{TX})}\right)^{\frac{2}{\alpha}}B\left(\frac{2}{\alpha},1-\frac{2}{\alpha}\right)\sum_{m_k=1}^{M_k}\rho_k(m_k)m_k^{1-2/\alpha}\right\}\end{aligned}\tag{38}$$

Defining $S=\sum_{k=1}^{K}S_k$ and $Z=I_0+\sum_{k=1}^{K}I_k$, then

$$\begin{aligned}\mathcal{P}_{\mathrm{cov}}(\beta) &\approx \Pr[S_0\geq\beta Z]+\Pr[S_0<\beta Z, S\geq\beta Z-S_0]\\ &= \Pr[S_0\geq\beta Z]+\Pr[S_0<\beta Z, S\geq\beta Z]\\ &\quad+\Pr[S_0<\beta Z,\beta Z-S_0<S\leq\beta Z]\end{aligned}\tag{41}$$

The first item $\Pr[S_0\geq\beta Z]$ can be easily calculated with the Laplace functions of I_k, i.e.,

$$\begin{aligned}\Pr[S_0\geq\beta Z] &\overset{(k)}{=}\sum_{m_0=0}^{M_0-2}\rho_0(m_0+1)\\ &\quad\times\int_0^{\infty}\prod_{k=0}^{K}\mathcal{L}_{I_k}\left(\frac{\beta(m_0+1)r^{\alpha}}{P_0^{(\mathrm{TX})}}\right)f_{r_0}(r)\mathrm{d}r,\end{aligned}\tag{42}$$

where (k) follows the exponential distribution of h_{x_0}. Since it is complex to get closed-form expression for the *pdf* of S_k and I_k by inverse Laplace transform. we apply the Gamma distribution [43] to approximate the distribution for S and Z. It is proved in [45] and [46] that second-order moment matching of Gamma is sufficient to approximate the distribution of sums of Gammas. Thus, the Gamma distribution with the same first and second order moments as S has the following shape parameter κ_S and scale parameter θ_S.

$$\kappa_S=\frac{\left(\sum\limits_{k=1}^{K}\mathbb{E}[S_k]\right)^2}{\sum\limits_{k=1}^{K}\mathbb{V}[S_k]},\theta_S=\frac{\sum\limits_{k=1}^{K}\mathbb{V}[S_k]}{\sum\limits_{k=1}^{K}\mathbb{E}[S_k]},\tag{43}$$

where $\mathbb{E}[S_k]$ and $\mathbb{V}[S_k]$ are the mean and variance of S_k. The mean of S_k can be obtained with (2-19) in [34]:

$$\begin{aligned}&\mathbb{E}[S_k]\\ &=\mathbb{E}\left[\sum_{x_k\in\Phi_k\cap\mathcal{B}(0,\chi_k)}\mathbb{1}(E_1\&E_2\&E_4)\frac{P_k^{(\mathrm{TX})}}{m_{x_k}+1}\|x_k\|^{-\alpha}h_{x_k}\right]\\ &=\frac{2\pi\lambda_k\omega_k\eta_kP_k^{(\mathrm{TX})}}{M_0}\frac{\chi_k^{2-\alpha}-d_0^{2-\alpha}}{2-\alpha}\sum_{m_k=0}^{M_k-1}\rho_k(m_k+1)\frac{M_0-m_k}{m_k+1},\end{aligned}\tag{44}$$

where $d_0=1$ is the reference distance at which the path loss fading is 1. With the result (2-21) in [34], the variance of S_k is

$$\begin{aligned}\mathbb{V}[S_k] &= E\left(h^2\right)\sum_{m_k=0}^{M_k-1}\rho_k(m_k+1)\frac{M_0-m_k}{M_0}\left(\frac{P_k^{(\mathrm{TX})}}{m_k+1}\right)^2\\ &\quad\times 2\pi\lambda_k\omega_k\eta_k\int_{d_0}^{\chi_k}r^{1-2\alpha}\mathrm{d}r\\ &=\frac{\pi\lambda_k\omega_k\eta_k\left(P_k^{(\mathrm{TX})}\right)^2}{M_0}\frac{\chi_k^{2-2\alpha}-d_0^{2-2\alpha}}{2-2\alpha}\\ &\quad\times\sum_{m_k=0}^{M_k-1}\rho_k(m_k+1)\frac{M_0-m_k}{(m_k+1)^2}.\end{aligned}\tag{45}$$

Similarly, the shape and scale parameters of the Gamma distribution with the same first and second order moments as Z are expressed as:

$$\kappa_Z=\frac{\left(\mathbb{E}[I_0]+\sum\limits_{k=1}^{K}\mathbb{E}[I_k]\right)^2}{\mathbb{V}[I_0]+\sum\limits_{k=1}^{K}\mathbb{V}[I_k]},\quad\theta_Z=\frac{\mathbb{V}[I_0]+\sum\limits_{k=1}^{K}\mathbb{V}[I_k]}{\mathbb{E}[I_0]+\sum\limits_{k=1}^{K}\mathbb{E}[I_k]},\tag{46}$$

where the mean and variance of I_0 conditioned on r_0 are

$$\begin{aligned}\mathbb{E}[I_0|r_0] &= \mathbb{E}\left[\sum_{x\in\Phi_0\setminus x_0}\mathbf{1}(\text{occupied})\frac{P_0^{(\mathrm{TX})}}{m_x}\|x\|^{-\alpha}h_x\right]\\ &=2\pi\lambda_0\sum_{m=1}^{M_0}\rho_0(m)\frac{P_0^{(\mathrm{TX})}}{M_0}\frac{r_0^{2-\alpha}}{\alpha-2},\end{aligned}\tag{47}$$

and

$$\mathbb{V}[I_0|r_0]=\frac{r_0^{2-2\alpha}}{2\alpha-2}\frac{\pi\lambda_0\left(P_0^{(\mathrm{TX})}\right)^2}{M_0}\sum_{m_k=1}^{M_k}\frac{\rho_0(m)}{m}.\tag{48}$$

The mean and variance of I_k are obtained as

$$\mathbb{E}[I_k]=\frac{2\pi\lambda_k\omega_kP_k^{(\mathrm{TX})}}{M_0}\frac{d_0^{2-\alpha}}{\alpha-2}\sum_{m_k=1}^{M_k}\rho_k(m_k),\tag{49}$$

and

$$\mathbb{V}[I_k] = \frac{d_0^{2-2\alpha}}{2\alpha-2}\frac{\pi\lambda_k\omega_k\left(P_k^{(\mathrm{TX})}\right)^2}{M_0}\sum_{m_k=1}^{M_k}\frac{\rho_k(m_k)}{m_k}. \quad (50)$$

With the Gamma approximation of S and Z, the probability $\Pr[S_0 < \beta Z, S \geq \beta Z]$ is approximately obtained as:

$$\begin{aligned}
&\Pr[S_0 < \beta Z, S \geq \beta Z] \\
&= \mathbb{E}_{m_0,r_0}\left\{\int_0^\infty\int_0^{\beta z}\int_{\beta z}^\infty f_S(s)\,ds\,f_{S_0}(x)\,dx\,f_I(z)\,dz\right\} \\
&\overset{(l)}{=} \mathbb{E}_{m_0,r_0}\left\{\int_0^\infty \frac{\Gamma\left(\kappa_S,\frac{\beta z}{\theta_S}\right)}{\Gamma(\kappa_S)}\left(1-e^{-\frac{m_0+1}{P_0^{(\mathrm{TX})}r_0^{-\alpha}}\beta z}\right)f_Z(z)\,\mathrm{d}z\right\} \\
&\overset{(m)}{=} \mathbb{E}_{m_0,r_0}\left\{\frac{\Gamma(\kappa_S+\kappa_Z)\varphi^{\kappa_S}\mathcal{Z}_3(1)}{\Gamma(\kappa_S)\Gamma(\kappa_Z+1)}\right\} \\
&\quad - \mathbb{E}_{m_0,r_0}\left\{\frac{\Gamma(\kappa_S+\kappa_Z)\varphi^{\kappa_S}}{\Gamma(\kappa_S)\Gamma(\kappa_Z+1)}\mathcal{Z}_3\left(1+\frac{\beta\theta_Z(m_0+1)}{P_0^{(\mathrm{TX})}r_0^{-\alpha}}\right)\right\}
\end{aligned} \quad (51)$$

where $\varphi = \frac{\beta\theta_Z}{\theta_S}$ and $\mathcal{Z}_3(x)$ is expressed as (31). (l) and (m) follow the Gamma distribution of S, Z and the exponential distribution of h_{x_0}. Similarly, the probability $\Pr[S_0 < \beta Z, \beta Z - S_0 < S \leq \beta Z]$ can be obtained as:

$$\begin{aligned}
&\Pr[S_0 < \beta Z, \beta Z - S_0 < S \leq \beta Z] \\
&\overset{(n)}{=} \mathbb{E}_{m_0,r_0}\left\{\int_0^\infty\int_0^{\beta z}\int_{\beta z-s}^{\beta z} f_{S_0}(x)\,dx\,f_S(s)\,ds\,f_Z(z)\,\mathrm{d}z\right\} \\
&= \mathbb{E}_{m_0,r_0}\left\{\frac{\Gamma(\kappa_S+\kappa_Z)\varphi^{\kappa_S}}{\Gamma(\kappa_Z)\Gamma(\kappa_S+1)}\mathcal{Z}_4(\varphi)\right\} \\
&\quad - \mathbb{E}_{m_0,r_0}\left\{\frac{\Gamma(\kappa_S+\kappa_I)\varphi^{\kappa_S}}{\Gamma(\kappa_S+1)\Gamma(\kappa_Z)}\mathcal{Z}_4\left(\varphi+\frac{\beta\theta_Z(m_0+1)}{P_0^{(\mathrm{TX})}r_0^{-\alpha}}\right)\right\}
\end{aligned} \quad (52)$$

where (n) is the result of the area transformation of the double integral and $\mathcal{Z}_4(x)$ is expressed as (32). Combining (41), (42), (51) and (52), the coverage probability can be approximated as (29).

REFERENCES

[1] N. Zhang, S. Zhang, S. Wu, J. Ren, J. W. Mark, and X. Shen, "Beyond coexistence: Traffic steering in LTE networks with unlicensed bands," *IEEE Wireless Commun.*, vol. 23, no. 6, pp. 40–46, Dec. 2016.

[2] N. Zhang, N. Cheng, A. Gamage, K. Zheng, J. W. Mark, and X. Shen, "Cloud assisted HetNets toward 5G wireless networks," *IEEE Commun. Mag.*, vol. 53, no. 6, pp. 59–65, Jun. 2015.

[3] Q. C. Li, H. Niu, A. T. Papathanassiou, and G. Wu, "5G network capacity: Key elements and technologies," *IEEE Veh. Technol. Mag.*, vol. 9, no. 1, pp. 71–78, Mar. 2014.

[4] D. Marabissi, G. Bartoli, R. Fantacci, and M. Pucci, "An optimized CoMP transmission for a heterogeneous network using eICIC approach," *IEEE Trans. Veh. Technol.*, vol. 65, no. 10, pp. 8230–8239, Oct. 2016.

[5] D. Lee *et al.*, "Coordinated multipoint transmission and reception in LTE-advanced: Deployment scenarios and operational challenges," *IEEE Commun. Mag.*, vol. 50, no. 2, pp. 148–155, Feb. 2012.

[6] S. Bassoy, H. Farooq, M. A. Imran, and A. Imran, "Coordinated multi-point clustering schemes: A survey," *IEEE Commun. Surveys Tuts.*, vol. 19, no. 2, pp. 743–764, 2nd Quart., 2017.

[7] G. Paschos, E. Baştuğ, I. Land, G. Caire, and M. Debbah, "Wireless caching: Technical misconceptions and business barriers," *IEEE Commun. Mag.*, vol. 54, no. 8, pp. 16–22, Aug. 2016.

[8] I. Atzeni, M. Maso, I. Ghamnia, E. Baştuğ, and M. Debbah. (May 2017). "Flexible cache-aided networks with backhauling." [Online]. Available: https://arxiv.org/abs/1705.08576

[9] S. Zhang, N. Zhang, S. Zhou, J. Gong, Z. Niu, and X. Shen, "Energy-aware traffic offloading for green heterogeneous networks," *IEEE J. Sel. Areas Commun.*, vol. 34, no. 5, pp. 1116–1129, May 2016.

[10] Z. Zheng, X. Zhang, L. X. Cai, R. Zhang, and X. Shen, "Sustainable communication and networking in two-tier green cellular networks," *IEEE Wireless Commun.*, vol. 21, no. 4, pp. 47–53, Apr. 2014.

[11] H. Holma and A. Toskala, *LTE-Advanced: 3GPP Solution for IMT-Advanced*. Hoboken, NJ, USA: Wiley, 2012.

[12] Y. Li, L. Bai, C. Chen, Y. Jin, and J. Choi, "Successive orthogonal beamforming for cooperative multi-point downlinks," *IET Commun.*, vol. 7, no. 8, pp. 706–714, May 2013.

[13] X. Tao, X. Xu, and Q. Cui, "An overview of cooperative communications," *IEEE Commun. Mag.*, vol. 50, no. 6, pp. 65–71, Jun. 2012.

[14] F. Baccelli and A. Giovanidis, "A stochastic geometry framework for analyzing pairwise-cooperative cellular networks," *IEEE Trans. Wireless Commun.*, vol. 14, no. 2, pp. 794–808, Feb. 2015.

[15] W. Nie, F.-C. Zheng, X. Wang, W. Zhang, and S. Jin, "User-centric cross-tier base station clustering and cooperation in heterogeneous networks: Rate improvement and energy saving," *IEEE J. Sel. Areas Commun.*, vol. 34, no. 5, pp. 1192–1206, May 2016.

[16] G. Nigam, P. Minero, and M. Haenggi, "Coordinated multipoint joint transmission in heterogeneous networks," *IEEE Trans. Commun.*, vol. 62, no. 11, pp. 4134–4146, Nov. 2014.

[17] G. Nigam, P. Minero, and M. Haenggi, "Spatiotemporal cooperation in heterogeneous cellular networks," *IEEE J. Sel. Areas Commun.*, vol. 33, no. 6, pp. 1253–1265, Jun. 2015.

[18] R. Tanbourgi, S. Singh, J. G. Andrews, and F. K. Jondral, "A tractable model for noncoherent joint-transmission base station cooperation," *IEEE Trans. Wireless Commun.*, vol. 13, no. 9, pp. 4959–4973, Sep. 2014.

[19] A. H. Sakr and E. Hossain, "Location-aware cross-tier coordinated multipoint transmission in two-tier cellular networks," *IEEE Trans. Wireless Commun.*, vol. 13, no. 11, pp. 6311–6325, Nov. 2014.

[20] H. Wu, X. Tao, N. Li, and J. Xu, "Coverage analysis for CoMP in two-tier HetNets with nonuniformly deployed femtocells," *IEEE Commun. Lett.*, vol. 19, no. 9, pp. 1600–1603, Sep. 2015.

[21] E. Baştuğ, M. Bennis, M. Kountouris, and M. Debbah, "Cache-enabled small cell networks: Modeling and tradeoffs," *EURASIP J. Wireless Commun. Netw.*, vol. 2015, no. 1, p. 41, Jan. 2015.

[22] C. Yang, Y. Yao, Z. Chen, and B. Xia, "Analysis on cache-enabled wireless heterogeneous networks," *IEEE Trans. Wireless Commun.*, vol. 15, no. 1, pp. 131–145, Jan. 2016.

[23] Y. Liu, C. Yand, Y. Yao, B. Xia, Z. Chen, and X. Li, "Interference management in cache-enabled stochastic networks: A content diversity approach," *IEEE Access*, vol. 5, no. 4, pp. 1609–1617, Feb. 2017.

[24] J. Liu and S. Sun, "Energy efficiency analysis of cache-enabled cooperative dense small cell networks," *IET Commun.*, vol. 11, no. 4, pp. 477–482, Mar. 2017.

[25] W. Wen, Y. Cui, F.-C. Zheng, S. Jin, and Y. Jiang. (Jan. 2017). "Random caching based cooperative transmission in heterogeneous wireless networks." [Online]. Available: https://arxiv.org/abs/1701.05761

[26] B. Blaszczyszyn and A. Giovanidis, "Optimal geographic caching in cellular networks," in *Proc. IEEE Int. Conf. Commun. (ICC)*, Jun. 2015, pp. 3358–3363.

[27] Y. Guo, L. Duan, and R. Zhang, "Cooperative local caching under heterogeneous file preferences," *IEEE Trans. Commun.*, vol. 656, no. 1, pp. 444–457, Jan. 2017.

[28] M. Afshang, H. S. Dhillon, and P. H. J. Chong, "Fundamentals of cluster-centric content placement in cache-enabled device-to-device networks," *IEEE Trans. Commun.*, vol. 64, no. 6, pp. 2511–2526, Jun. 2016.

[29] H. S. Dhillon, Y. Li, P. Nuggehalli, Z. Pi, and J. G. Andrews, "Fundamentals of heterogeneous cellular networks with energy harvesting," *IEEE Trans. Wireless Commun.*, vol. 13, no. 5, pp. 2782–2797, May 2014.

[30] P.-S. Yu, J. Lee, T. Q. S. Quek, and Y.-W. P. Hong, "Traffic offloading in heterogeneous networks with energy harvesting personal cells-network throughput and energy efficiency," *IEEE Trans. Wireless Commun.*, vol. 15, no. 2, pp. 1146–1161, Feb. 2016.

[31] F. Parzysz, M. Di Renzo, and C. Verikoukis, "Power-availability-aware cell association for energy-harvesting small-cell base stations," *IEEE Trans. Wireless Commun.*, vol. 16, no. 4, pp. 2409–2422, Apr. 2017.
[32] J. Gong, S. Zhou, and Z. Zhou, "Networked MIMO with fractional joint transmission in energy harvesting systems," *IEEE Trans. Commun.*, vol. 64, no. 8, pp. 3323–3336, Aug. 2016.
[33] Y.-H. Chiang and W. Liao, "Green multicell cooperation in heterogeneous networks with hybrid energy sources," *IEEE Trans. Wireless Commun.*, vol. 15, no. 12, pp. 7911–7925, Dec. 2016.
[34] F. Baccelli and B. Blaszczyszyn, *Stochastic Geometry and Wireless Networks: Theory*, vol. 1. Hanover, MA, USA: Now Publishers, 2009.
[35] X. Wang, M. Chen, T. Taleb, A. Ksentini, and V. C. M. Leung, "Cache in the air: Exploiting content caching and delivery techniques for 5G systems," *IEEE Commun. Mag.*, vol. 52, no. 2, pp. 131–139, Feb. 2014.
[36] J.-S. Ferenc and Z. Néda, "On the size distribution of poisson Voronoi cells," *Phys. A, Statist. Mech. Appl.*, vol. 385, no. 2, pp. 519–529, 2007.
[37] T. Kiang, "Random fragmentation in two and three dimensions," *Zeitschrift Astrophys.*, vol. 64, pp. 433–439, Jun. 1966.
[38] H. S. Dhillon and J. G. Andrews, "Downlink rate distribution in heterogeneous cellular networks under generalized cell selection," *IEEE Wireless Commun. Lett.*, vol. 3, no. 1, pp. 42–45, Feb. 2014.
[39] M. Di Renzo, W. Lu, and P. Guan, "The intensity matching approach: A tractable stochastic geometry approximation to system-level analysis of cellular networks," *IEEE Trans. Wireless Commun.*, vol. 15, no. 9, pp. 5963–5983, Sep. 2016.
[40] S. Gradshteyn and I. M. Ryzhik, *Table of Integrals, Series, and Products*. 6th ed. New York, NY, USA: Academic, 2000.
[41] M. Di Renzo, A. Guidotti, and G. E. Corazza, "Average rate of downlink heterogeneous cellular networks over generalized fading channels: A stochastic geometry approach," *IEEE Trans. Commun.*, vol. 61, no. 7, pp. 3050–3071, Jul. 2013.
[42] L. Bai, L. Zhu, J. Choi, F. Liu, and Q. Yu, "Cooperative transmission over Rician fading channels for geostationary orbiting satellite collocation system," *IET Commun.*, vol. 11, no. 4, pp. 538–547, Mar. 2017.
[43] R. W. Heath, M. Kountouris, and T. Bai, "Modeling heterogeneous network interference using poisson point processes," *IEEE Trans. Signal Process.*, vol. 61, no. 16, pp. 4114–4126, Aug. 2013.
[44] R. W. Heath, Jr., T. Wu, Y. H. Kwon, and A. C. K. Soong, "Multiuser MIMO in distributed antenna systems with out-of-cell interference," *IEEE Trans. Signal Process.*, vol. 59, no. 10, pp. 4885–4899, Oct. 2011.

Huici Wu received the B.S. degree in information engineering from the Communication University of China, Beijing, China, in 2013. She is currently pursuing the Ph.D. degree in communications and information systems with the Beijing University of Posts and Telecommunications, Beijing, China. From 2016 to 2017, she was visiting the Broadband Communications Research Group with the Department of Electrical and Computer Engineering, University of Waterloo, Waterloo, ON, Canada. Her research interests are in the area of wireless communications and networks, with current emphasis on the cooperation and physical layer security in heterogeneous networks.

Xiaofeng Tao (SM'13) received the B.S. degree in electrical engineering from Xi'an Jiaotong University, Xi'an, China, in 1993, and the M.S.E.E. and Ph.D. degrees in telecommunication engineering from the Beijing University of Posts and Telecommunications (BUPT), Beijing, China, in 1999 and 2002, respectively.

He was the Chief Architect of the Chinese National FuTURE Fourth-Generation (4G) TDD working group from 2003 to 2006, established the 4G TDD CoMP trial network in 2006, and a Visiting Professor with Stanford University, Stanford, CA, USA, from 2010 to 2011. He is currently a Professor with the BUPT and a fellow of the Institution of Engineering and Technology. He is currently the inventor or co-inventor of 50 patents and the author or co-author of 120 papers in 4G and beyond 4G.

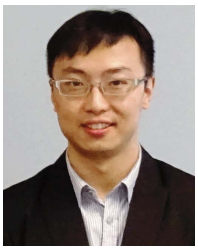

Ning Zhang (M'15) received the Ph.D. degree from the University of Waterloo in 2015. He is currently an Assistant Professor with the Department of Computing Science, Texas A&M University-Corpus Christi. Before that, he was a Post-Doctoral Research Fellow with the BBCR laboratory, University of Waterloo. His current research interests include next generation wireless networks, software defined networking, vehicular networks, and physical layer security. He was a co-recipient of the Best Paper Award at the IEEE GLOBECOM 2014 and the IEEE WCSP 2015.

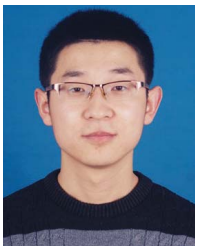

Danyang Wang received the B.S. degree in communications engineering from Xidian University, Xi'an, China, in 2012. He is currently pursuing the Ph.D. degree with the State Key Laboratory of Integrated Service Networks, School of Telecommunications Engineering, Xidian University, Xi'an. His research interests include cognitive radio networks, cooperative spectrum sensing, and NOMA.

Shan Zhang (S'13–M'16) received the B.S. degree from the Department of Information, Beijing Institute Technology, Beijing, China, and the Ph.D. degree from the Department of Electronic Engineering, Tsinghua University, in 2011 and 2016, respectively. She is currently a Post-Doctoral Fellow with the Department of Electronic and Computer Engineering, University of Waterloo, Waterloo, ON, Canada. Her research interests include resource and traffic management for green communication, intelligent vehicular networking, and software defined networking. She was a recipient of the Best Paper Award at the Asia-Pacific Conference on Communication in 2013.

Xuemin (Sherman) Shen (M'97–SM'02–F'09) received the B.Sc. degree from Dalian Maritime University, China, in 1982, and the M.Sc. and Ph.D. degrees from Rutgers University, Middlesex County, NJ, USA, in 1987 and 1990, respectively, all in electrical engineering. He is currently a University Professor and the Associate Chair for Graduate Studies, Department of Electrical and Computer Engineering, University of Waterloo, Waterloo, ON, Canada. He research focuses on resource management, wireless network security, social networks, smart grid, and vehicular ad hoc and sensor networks. He was an elected member of the IEEE ComSoc Board of Governor, and the Chair of Distinguished Lecturers Selection Committee. He was a recipient of the Excellent Graduate Supervision Award in 2006, and the Premiers Research Excellence Award in 2003 from the Province of Ontario, Canada. He served as the Technical Program Committee Chair/Co-Chair for the IEEE Globecom16, Infocom14, the IEEE VTC10 Fall, and Globecom07, the Symposia Chair for the IEEE ICC10, the Tutorial Chair for the IEEE VTC11 Spring, and the IEEE ICC08, the General Co-Chair for ACM Mobihoc15, Chinacom07, and QShine06, the Chair for the IEEE Communications Society Technical Committee on Wireless Communications, and P2P Communications and Networking. He also serves/served as the Editor-in-Chief for the IEEE INTERNET OF THINGS JOURNAL, the *IEEE Network Magazine*, *Peer-to-Peer Networking and Application*, and the IET *Communications*; a Founding Area Editor for the IEEE TRANSACTIONS ON WIRELESS COMMUNICATIONS; an Associate Editor for the IEEE TRANSACTIONS ON VEHICULAR TECHNOLOGY, *Computer Networks*, and the ACM/Wireless Networks, etc.; and the Guest Editor for the IEEE JSAC, the IEEE WIRELESS COMMUNICATIONS, the *IEEE Communications Magazine*, and *ACM Mobile Networks and Applications*, etc. He is currently a registered Professional Engineer of Ontario, Canada, an Engineering Institute of Canada Fellow, a Canadian Academy of Engineering Fellow, a Royal Society of Canada Fellow, and a Distinguished Lecturer of the IEEE Vehicular Technology Society and Communications Society.